

Adsorption of methane on bundles of closed-ended single-wall carbon nanotubes

S. Talapatra and A. D. Migone

Department of Physics, Southern Illinois University, Carbondale, Illinois 62901

(Received 2 July 2001; published 7 January 2002)

The results of an adsorption isotherm investigation of methane on closed-ended single-wall nanotube bundles are presented. The isosteric heat of adsorption was determined as a function of the amount of methane adsorbed on the SWNT substrate for coverages in the first layer. The isosteric heat of adsorption is found to decrease with increasing coverage. This behavior provides an explanation for differences in previously reported values for this quantity. Substantial agreement was found between this study and previous reports on the temperature dependence of the pressures at which the two first-layer substeps occur for methane adsorbed on SWNT bundles. There was, however, one exception: we found no evidence suggesting the existence of a phase transition around 90 K in the high pressure substep. We put forth a possible explanation for this difference.

DOI: 10.1103/PhysRevB.65.045416

PACS number(s): 61.48.+c, 05.70.Np, 68.47.-b

I. INTRODUCTION

Currently, there is a great deal of interest in the study of the adsorption of gases on carbon nanotubes. The number of theoretical,¹⁻⁷ simulational,⁸⁻¹¹ and experimental¹²⁻²⁶ investigations of these systems continues to increase at a rapid pace. This interest is motivated by fundamental as well as by practical considerations. Simple molecular or monoatomic gases adsorbed on single-wall nanotube bundles can provide good experimental realizations of matter in one dimension.^{2,14,16,21-23} At the same time, because they are mostly “surface,” carbon nanotubes can prove to be excellent adsorbent materials; there is considerable interest in their potential use for the storage of hydrogen²⁴⁻²⁷ and other fluids.

Closed-ended carbon nanotube bundles have three different groups of sites which may be available for adsorption.^{5,8} They are the outer surfaces of those tubes located on the outside surface of the bundles (outer sites), the “grooves” formed by the space where two of these outer tubes come in close proximity lying side by side parallel to one another (groove sites), and, finally, the interstitial channels (IC) at the interior of the bundles. The first two of these three groups of sites are always available for adsorption, regardless of the size of the adsorbate species. The binding energies in the groove sites is higher than that in the outer sites because there is a greater number of C neighbors close to each groove site.⁵ Whether a particular species can adsorb or not on the IC sites depends on the size of the adsorbate relative to the effective diameter of the IC.⁵

Methane adsorbed on closed-ended single-wall carbon nanotubes has previously been studied by adsorption isotherms¹³ and by adsorption isotherms and calorimetry.¹⁸ The adsorption isotherm study focused on low coverage adsorption at relatively high temperatures (between 155 and 195 K).¹³ In that study the binding energy for methane on the highest binding energy sites on the nanotube bundles was determined from the value of the low coverage isosteric heat of adsorption. A value approximately 70% higher than that on planar graphite was found on these sites. In a related study, it was concluded that methane is too large to be able to occupy the IC sites.¹²

The combined isotherm and calorimetry study¹⁸ focused

on more extended adsorption isotherms, and, on the determining the binding energy for methane both from isosteric heat and from differential heat of adsorption measurements. This study found that full monolayer isotherms display two rounded substeps. The lower pressure (higher binding energy) substep was identified as indicating adsorption on the IC sites. The higher pressure substep was identified as corresponding to adsorption on the outer sites.¹⁸ The values of the binding energy of the lower coverage step, derived both from the isosteric heat determinations as well as from the differential heat of adsorption measurements, were 20% larger than those for methane on planar graphite. This study also found evidence of the presence of a phase transition in the outer sites (i.e., on the higher coverage substep) at a temperature between 87 and 90 K, significantly higher than the monolayer critical point for methane on planar graphite. The nature of this transition was not identified.¹⁸

In the isotherm and calorimetric study, only two groups of possible adsorption sites on the SWNT bundles were considered when interpreting the observed isotherm features: the outer sites and the IC sites.¹⁸ The grooves were not considered in this interpretation. This has resulted in disagreement surrounding the identification of the sites on which the lower pressure adsorption substep occurs.^{12,18} By contrast with the lower pressure substep, no disagreement exists regarding the identification of the second, higher coverage, higher pressure substep: it corresponds to adsorption occurring on the outer sites.^{14,18}

In this paper we present the results of an adsorption isotherm investigation of methane on closed-ended single-wall nanotubes (SWNT's) consisting of measurements conducted for temperatures in the range between 69 to 129 K. The coverages investigated in these isotherms extend up to the top of the second rounded substep. The low coverage data is compared to the high-temperature, low-coverage data which was used to determine the isosteric heat and binding energy in a previous study.^{12,13} The isosteric heat values are also examined as a function of coverage. A comparison is made between the coverage dependence of the isosteric heat and the two different values for this quantity which have been reported in the literature.^{12,13,18} The pressures of the two rounded steps, which were first reported in the isotherm and calorimetric study,¹⁸ are compared to the corresponding fea-

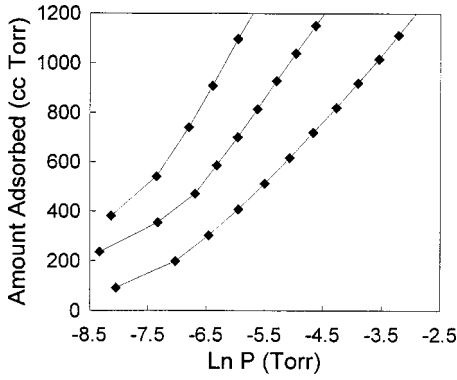


FIG. 1. Low-coverage adsorption isotherm data for the three highest temperatures investigated in this study (from left to right: 108.98, 117.87, and 129.90 K). The amount of methane adsorbed, in cc Torr (1 cc Torr = 3.54×10^{16} molecules) is plotted as a function of the logarithm of the pressure, in Torr. For lower temperatures, the pressures in this low coverage region start falling below the resolution limit of our setup. One full layer covering the SWNT bundles corresponds to a coverage of approximately 5500 cc Torr.

tures found in our data. Finally, the region in which a phase transition was identified around 90 K in the combined isotherm and calorimetric study¹⁸ is investigated and, an explanation for the differences between the observations in the present study and those in a prior report¹⁸ is provided.

II. EXPERIMENTAL

The sample used in these measurements was single-wall nanotubes prepared by the arc-discharge method²⁸ by C. Journet in Professor Bernier's laboratory in Montpellier. Samples from this same source were used in previous studies from our laboratory.^{12-14,16} The nanotubes were not subjected to any post-production treatment.

The automated adsorption setup used in these measurements has been described in greater detail elsewhere.²⁹ Thermomolecular corrections, following the prescriptions of Takaiishi and Sensui,³⁰ were applied to the data.

The methane gas used in these measurements was research purity grade (99.999%) produced by Matheson Gas Products, Inc. The waiting times for each data point in our measurements ranged from 16 000 seconds (at the lowest coverages and temperatures) to 6000 seconds per data point (at higher pressures and temperatures).

III. RESULTS AND DISCUSSION

A. Low coverage results

Figure 1 presents the lower coverage portion for the three higher temperature isotherms investigated in this study (108.94, 117.87, and 129.90 K). The data displayed goes only up to 1200 cc Torr. For reference, one full monolayer covering the entire nanotube bundles (i.e., the completion of a layer on the outer sites, corresponding to the top of the second rounded substep in the isotherms, see Fig. 4 below) occurs at a coverage of approximately 5500 cc Torr.

In a previous study¹² we used data between, approximately, 2 and 10% of one full monolayer on the nanotube

bundles for the determination of the isosteric heat of the adsorbate for a range of temperatures higher than those reported here. The binding energy of an adsorbate to a substrate can be extracted from the isosteric heat, provided that the adsorbed gas behaves as a reduced dimensionality ideal gas on the substrate.² This restriction requires that only low coverage isosteric heat values be used in the determination of the binding energy.

The isosteric heat of adsorption is defined as³¹

$$q_{st} = -k_B T^2 (\partial \ln P / \partial T)_n. \quad (1)$$

Here, n is the amount of gas adsorbed on the nanotube substrate, P the pressure of the coexisting three-dimensional vapor, k_B is Boltzmann's constant, and T the temperature at which the isotherm is measured.

It is clear from Eq. (1) that, for a fixed amount of gas adsorbed on a substrate, the isosteric heat of adsorption can be determined from the slope of the plot of $\ln P$ at that coverage, as a function of $1/T$. Figure 2 presents such plots: $\ln P$ vs $1/T$ is plotted for all the features investigated in this study. Figure 2 is a summary of the findings of this report.

The lowest line in Fig. 2 corresponds to the data used to compute the isosteric heat at low coverages (300 cc Torr) and higher temperatures in a previous study,^{12,13} plus the data corresponding to the two highest isotherms measured in this study, and an additional data point from a previously unreported measurement at 143.82 K. The second lowest line corresponds to the pressure at the midpoint of the lower coverage substep in the first layer. The second line from the top corresponds to the pressure at the midpoint coverage of the first layer for methane on planar graphite³² (presented here just for comparison). And, the topmost line corresponds to the pressure at the midpoint of the higher coverage substep in the first layer of methane on SWNT bundles. The two sets of symbols used correspond to our results (filled) and the isotherm results from the combined calorimetric and adsorption study¹⁸ (open).

We discuss the lowest curve in Fig. 2, next. The points corresponding to the lower temperature isotherms (i.e., the result of the measurements conducted in this study) follow reasonably well the same line as those from the higher-temperature measurements.^{12,13} This confirms our previous determination of the isosteric heat values. If the isosteric heat is obtained from data displayed in the lower curve in Fig. 2 (including the new, lower temperature points), we obtain a value of 250 meV. This value is within 5% of the isosteric heat value determined in our previous report.^{12,13}

The fact that the isosteric heat determination presented here, as well as those performed in the previous high-temperature study,^{12,13} correspond to amounts adsorbed smaller than 10% of the amount required for the formation of a complete layer on the bundle, while those in the combined adsorption and calorimetric study¹⁸ involve coverages which are approximately three times larger, provides the most likely explanation for the difference in the reported isosteric heat values.^{12,13,18} In Fig. 3 we present a plot of the isosteric heat as a function of coverage. We find that the isosteric heat is a decreasing function of coverage. This result is in agreement

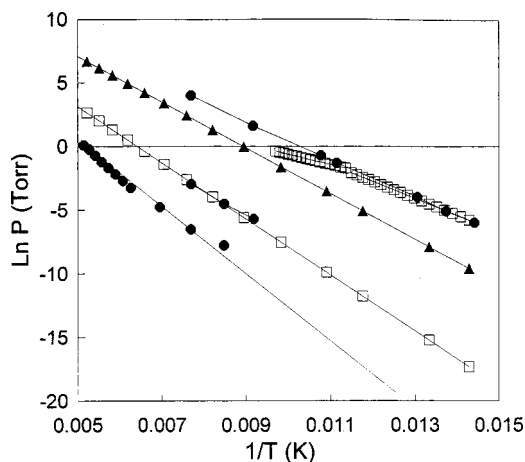


FIG. 2. Plot of the logarithm of the pressure as a function of the inverse of the temperature for different features in the adsorption data. The circles in the lowest curve correspond to the pressures at a coverage of 300 cc Torr. The high-temperature points in this curve were data reported previously (Refs. 12 and 13) and the lower temperature data was measured in this study, in addition, the result of an isotherm measurement at 143.82 K is also included. The slope of this curve, as is discussed in the text, corresponds to the isosteric heat of adsorption for this coverage. The second line from the bottom corresponds to the lower pressure substep: open squares are calculated using the $\ln P$ vs $1/T$ coefficients for this feature given in Ref. 18, while the full circles correspond to our data at 1200 cc Torr (i.e., in the region of the lower pressure substep in this study). The second line from the top corresponds to the pressure values at the midpoint coverage for monolayer methane on planar graphite; the filled triangles are calculated using the coefficients for this feature given in Ref. 32. This line is shown to provide a graphical comparison between adsorption on the SWNT bundles and adsorption on graphite. The top line corresponds to the pressure for the higher-pressure substep in the data for methane on SWNT bundles. The filled circles are the pressures corresponding to a coverage of 4000 cc Torr in our data. The open squares were calculated with the two sets of coefficients given in Ref. 18 for temperatures above and below 90 K.

with findings for other adsorbates,²⁰ in particular N_2 and H_2 , on the same type of SWNT substrates.

B. First substep region

Figure 4 displays data corresponding to the two rounded substeps present in the first layer of the film adsorbed on the SWNT bundle substrate. The lower coverage rounded substep present in the isotherms is only shown for the highest temperatures studied here.

The presence of two rounded substeps in the monolayer adsorption data of methane on SWNT bundles was first noted in the combined adsorption and calorimetry study of this system.¹⁸ The fact that the lower pressure, lower coverage substep occurs at pressure values which are lower than those corresponding, for the same temperature, on planar graphite was also noted in that study.¹⁸

Since lower pressures correspond to stronger binding to the substrate, that study concluded that the low-pressure broad substep corresponded to adsorption on the interstitial

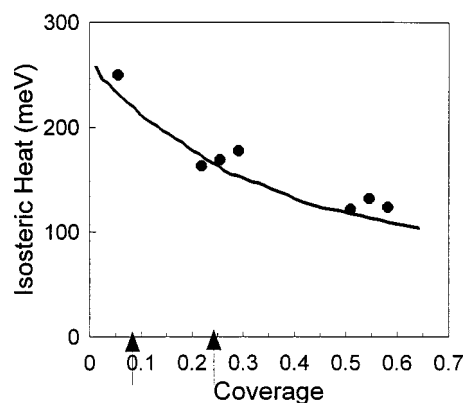


FIG. 3. Values of the isosteric heat of adsorption determined as a function of the amount of methane adsorbed on the bundles ($n = 1$ corresponds to a coverage of 5500 cc Torr). Arrows on the horizontal axis denote the location at which the low coverage data was determined in Ref. 12 and 13; and, the region that corresponds to the first step, which was the one used in Ref. 18 for the calculation of the isosteric heat. The low coverage isosteric heat was calculated using all the data (except for the lowest temperature) shown in Fig. 2. The rest of the values shown were calculated from the three or four highest temperature isotherms measured in this study. The limited statistics are responsible for the noise; however the trend in the data is clear.

channels.¹⁸ This interpretation is different from the one we have proposed in a recent comparative adsorption study of Xe, Ne, and CH_4 on the same substrate.¹² In our study, we concluded that no adsorption occurred in the IC sites for any one of these three gases.¹²

It is not our purpose to discuss in detail the issue of IC adsorption here. However, in what follows we provide a summary of the difference in interpretation of the low temperature data. It should be noted that this is a difference centered purely on interpretation, not on discrepancies be-

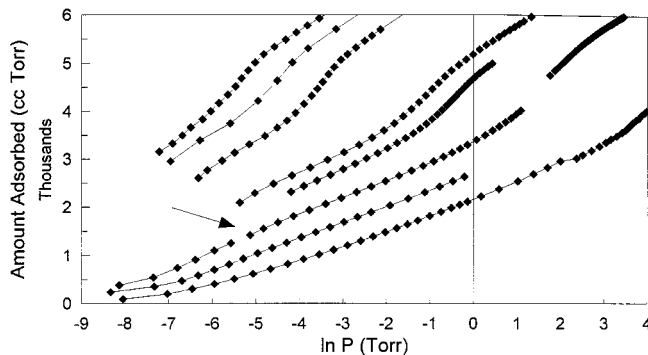


FIG. 4. Adsorption isotherm data for temperatures investigated in this study. From left to right: 69.41, 72.80, 76.51, 89.72, 92.83, 108.94, 117.87, and 129.90 K. The amount of methane adsorbed (in cc Torr) is given as a function of the logarithm of the equilibrium pressure, in Torr. A broad low-pressure substep can be seen in the data for 108.94 and 117.87 K. The top of this substep is marked by the arrow. The second, higher pressure substep is shown for all temperatures (except 117.87 K). At the lowest temperatures studied here, the completion of the higher-pressure step occurs near 5500 cc Torr.

tween data sets (to the contrary, the agreement between this study and the low pressure data in Ref. 18 is remarkably good, as we show below).

The authors of the combined isotherm and calorimetric study¹⁸ interpreted their data assuming that the only sites present in the SWNT bundles were the IC sites and outer sites. They failed to consider the existence of another group of high-energy binding sites on the nanotube bundles, namely, those on the groove sites.¹⁸ Additionally, they found that the size of the two steps was roughly comparable, and argued that this corresponded with calculations for the amount adsorbed on the IC's and on the outer surface for bundles of 37 tubes.¹⁸

A recent study by Cole's group⁸ has identified the formation of three separate phases, as a function of increasing coverage, as the outer surface of the bundles fills up. First, a row of atoms forms in the grooves; then, two rows of atoms parallel to the row already on the groove sites, form on the outer sites (this is the "three-channel" phase); and, finally, a full monolayer completes forming on the outer sites ("six-channel" phase). The calculations were done for atomic adsorbates (Ar and Kr) similar in size to methane on ideal bundles of nanotubes. In a real SWNT bundle substrate, it is likely that the boundaries between the three phases observed in the simulations will be blurred. Thus, conclusions derived from comparing the relative sizes of the first and second steps are problematic.

The full isotherm measurements¹⁸ were conducted at temperatures where the pressures for groove adsorption are extremely low. Under these circumstances, it is likely that an important fraction of the coverage corresponding to the three-channel phase contributed to the lower pressure step, again complicating the identification of the size of this feature.

All three groups of sites were considered in our comparative adsorption study.¹² The possibility of adsorption in the IC's was rejected as a result of comparing the specific areas obtained on the same substrate using two different adsorbates (Ne and Xe), and, of comparing the binding energy values determined for Ne, CH₄, and Xe.^{12,14} We measured the binding energy values for xenon, methane, and neon on SWNT bundles. We obtained, in all three cases, values for this quantity that were larger by about 70% than the values on planar graphite.¹² This indicates that the three adsorbates are occupying the same type of sites on the SWNT bundles. We measured the effective surface area of the same SWNT substrate using Xe and Ne and obtained the same result with both gases. Since these two different adsorbates gave approximately the same areas, and since Xe is too large to fit in the IC's, we concluded that neither one went into IC sites.^{12,14}

The groove sites present a reasonably uniform set of binding energies, and adsorption on them will result in a more or less sharp substep occurring in the isotherm data.^{5,8,12,14,18} Since the groove sites have deeper energy wells than the surface of planar graphite,^{8,9} this adsorption substep will occur at pressures lower than those corresponding to monolayer formation on planar graphite, at the same temperature.

An interpretation in terms of adsorption on the grooves and on the outer sites accounts very well for all the experimental data.^{14,18}

There can be some argument regarding whether small adsorbates can or cannot go into the IC's of nanotube bundles. There can be, as well, some argument regarding whether or not a small fraction of a given adsorbate, even for larger molecules, can occupy sites on especially large IC's which may result from the spread in diameters of the individual tubes within a bundle. However, there can be no argument regarding the fact that the groove sites and the outer sites are available for adsorption by methane molecules; and, that the groove sites are stronger binding sites than those present on planar graphite while the outer sites are weaker. Both grooves and outer sites *need* to be considered when explaining adsorption by methane on SWNT bundles.

The second lowest line in Fig. 2 corresponds to the plot of the midpoint pressure at the lower pressure step, presented as a function of the temperature. The two sets of symbols used in the figure correspond to our results (filled circles) and the isotherm results from the combined calorimetric and adsorption study¹⁸ (open symbols). It is clear that there is very good agreement between the two sets of experimental results with regards to the location of the midpoint of the lower pressure site, as the two data sets essentially coincide.

Note that the agreement found between the two sets of data, taken together with the coverage dependence of the isosteric heat data presented in Fig. 3, demonstrate that, when the same range of coverages are used for the calculation of the isosteric heat of adsorption, the same values for this quantity are obtained. The coverage dependence of the isosteric heat, thus, is the source of the difference in the reported values for this quantity.^{12,13,18}

Interestingly, the sample treatment prior to the adsorption measurements was quite different for both sets of measurements. The combined calorimetric and adsorption study¹⁸ employed heating under vacuum at 773 K while the present study involved extended evacuation at room temperature. It would appear, from the results displayed in Fig. 4 and especially from the overlapping regions in Fig. 2, that these differences in sample treatment had little measurable effect on the adsorption characteristics. This could suggest that either treatment method is sufficient. On the other hand, it is possible that higher substrate heating temperatures are required to produce a significant effect in the adsorption behavior.

C. Second substep region

At coverages above 2000 cc Torr the data of Fig. 4 corresponds to the region of the second rounded substep. This second rounded step was identified in the combined adsorption and calorimetry study¹⁸ as corresponding to the completion of a monolayer on the outer sites. We concur with this interpretation.

The temperatures displayed range from 69.41 to 129.90 K. All of these temperatures fall above the monolayer critical temperature for methane adsorbed on planar graphite 68.70 K. The degree of sharpness of these steps can be studied quantitatively by determining the difference in chemical po-

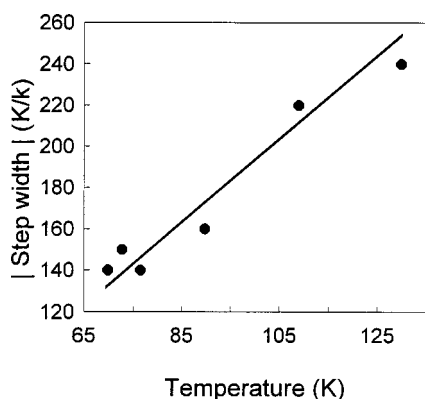


FIG. 5. The absolute value of the substep width, in chemical potential, of the higher pressure step is plotted as a function of temperature. The step width is calculated by taking the difference between the chemical potential at the top and bottom of the step. The increase in step width with increasing temperature is characteristic of measurements conducted above the critical point.

tential between the top and bottom of the rounded substep as a function of temperature. Figure 5 displays a plot of this step width as a function of temperature. It is clear that for the entire temperature range investigated the steps are all quite broad. The step width increases significantly with increasing temperature.

In Fig. 2, the data corresponding to the second substep in the isotherms is the top line. Again, our data points correspond to the full symbols while the open symbols correspond to previously reported data.¹⁸ For the higher temperatures, we have extrapolated pressure values using the coefficients for the expression of $\ln P$ as a function of $1/T$ given in Ref. 18.

Two features are evident in the two sets of data. First, the low temperature portion on both sets of data agree very well. Second, contrary to what has been reported before,¹⁸ we find no evidence of any high-temperature transition (indicated by a sharp change of slope in the open symbols plotted in Fig. 2) near 90 K.

We note that the data in this study and that from the previous report¹⁸ were not measured in the same manner. We measured full isotherms, and we obtained the pressure value corresponding to a fixed coverage, which at low temperatures coincides with the middle of the second rounded substep (approximately 4000 cc Torr), from them. In the report of the combined adsorption and calorimetric study,¹⁸ the temperature dependence of the equilibrium pressure at constant coverage was measured between 80 and 110 K at amounts adsorbed corresponding to the midpoint of the second substep, without measuring full adsorption isotherms. Details of how this was done were not provided.¹⁸ If the procedure followed in that study was to place an amount of gas in the cell, and then change the cell temperature while monitoring the pressure, problems could have followed. The only way to maintain the coverage constant while changing the cell temperature is to add an appropriate amount of methane after each temperature increase. If this is not done, the measurements are not performed at constant coverage, rather they are done as a function of a coverage that decreases with increas-

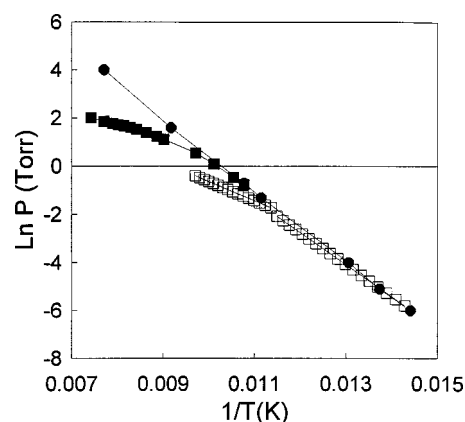


FIG. 6. Detailed view of the topmost curve shown in Fig. 2. Filled circles correspond to pressures measured in this study at a constant coverage of 4000 cc Torr. The two lines of open squares are calculated using the $\ln P$ vs $1/T$ coefficients for the second substep for temperatures above and below 90 K. The filled squares correspond to values of the pressure measured in our test run with the total number of molecules in the adsorption setup constant, starting from a coverage of 4000 cc Torr at 92 K, and increasing the temperature. Because of desorption, as the temperature of the SWNT's is increased, the coverage decreases along this path. Note the similarity between this plot and the open squares plot.

ing temperature. There is no indication how the addition of gas was done in the previous study.¹⁸ Problems with this process could explain the bend in the data.

To test whether this procedural difference could produce the difference observed in the data we conducted the following experiment. We dosed an amount adsorbed equal to 4000 cc Torr in the cell starting at 92 K. We waited for equilibrium to be reached. Then, while keeping the total amount of gas in the adsorption setup fixed (i.e., fixing the combined amount in the low-temperature cell plus that in the room temperature dosing volume), we increased the temperature of the cell, while leaving the valve between the cell and the dosing volume open.

The results of these measurements are displayed in Fig. 6, in which we present our constant coverage results (filled circles and straight line), determined from the adsorption isotherms at a coverage of 4000 cc Torr, the pressures calculated using the two linear regression formulas in Ref. 18 over the appropriate temperature ranges (open circles); and, the results of the test run with a fixed amount in the complete adsorption setup, i.e., cell plus dosing unit, with the valve between the cell and the dosing volume open (filled squares). This last curve shows a bend. Qualitatively, our run with a fixed amount of gas in the gas handling system is very similar to the second substep data in Ref. 18 (open symbols in Fig. 6).

We note that in the apparent bend in the slope occurs near 100 K in our run, whereas it occurs near 90 K in Ref. 18. The relative importance of desorption, which is responsible for the slope change in our measurements, will depend on details of the experimental setup (i.e., on the volume of the low temperature cell and on the amount of substrate used). In Ref. 18 only 0.026 g of SWNT sample were used, while we used approximately eight times more SWNT substrate in our measurements.

At lower temperatures, the data from both experiments agrees quite well. As the temperature is increased, the two sets increasingly disagree. If our experiment correctly represents what occurred, the temperature evolution of this disagreement can be readily understood. At lower temperatures the amount of methane in the vapor phase is negligible and hence both experiments proceed at essentially constant coverage. As the temperature increases so does the fraction of methane desorbed, hence the data in only one of the sets is measured at constant coverage while in the other the coverage is decreasing with increasing T , hence the growing difference.

IV. CONCLUSION

We have mapped out a significant portion of the phase diagram of the first layer of methane adsorbed on closed-ended SWNT bundles. We have determined the values of the isosteric heat of adsorption of this gas on the SWNT substrates as a function of coverage. Our data provides an explanation on the difference in isosteric heat values^{12,13,18} reported for this system: they are the result of the different coverage ranges explored in the different studies.

We have found a substantial degree of agreement with the

location of the first and second rounded substeps in the adsorption data previously reported for this system (with one exception, noted below).¹⁸ The interpretations of the nature of the lower pressure substep, however, remain different.^{12,18}

In this study we found no evidence of the presence of a high-temperature phase transition in the second step.¹⁸ We provide a possible explanation for this difference.

ACKNOWLEDGMENTS

We would like to thank Professor Oscar E. Vilches for several illuminating discussions and for sharing with us some of his results prior to publication. We have greatly benefitted from numerous conversations and exchanges, with Professor M. W. Cole, Dr. S. Gatica, and Dr. M. M. Calbi; we also want to express our thanks to them for making their results available to us prior to publication. A. D. M. would like to acknowledge support by the Research Corporation to the donors of the Petroleum Research Fund of the American Chemical Society for partial support of this work, and to the National Science Foundation through Grant No. DMR-0089713 for supporting this work. S. T. would like to acknowledge the support of the Link Foundation.

-
- ¹G. Stan, M. Boninsegni, V. H. Crespi, and M. W. Cole, *J. Low Temp. Phys.* **113**, 393 (1998).
- ²G. Stan, S. M. Gatica, M. Boninsegni, S. Curtarolo, and M. W. Cole, *Am. J. Phys.* **67**, 1170 (1999).
- ³S. M. Gatica, G. Stan, M. M. Calbi, J. K. Johnson, and M. W. Cole, *J. Low Temp. Phys.* **120**, 337 (2000).
- ⁴S. M. Gatica, M. W. Cole, G. Stan, J. M. Hartman, and V. H. Crespi, *Phys. Rev. B* **62**, 9989 (2000).
- ⁵G. Stan, M. J. Bojan, S. Curtarolo, S. M. Gatica, and M. W. Cole, *Phys. Rev. B* **62**, 2173 (2000).
- ⁶V. V. Simonyan, J. K. Johnson, A. Kuznetsova, and J. T. Yates, *J. Chem. Phys.* **114**, 4180 (2001).
- ⁷V. V. Simonyan, P. Diep, and J. K. P. Johnson, *J. Chem. Phys.* **111**, 9778 (1999).
- ⁸S. M. Gatica, M. J. Bojan, G. Stan, and M. W. Cole, *J. Chem. Phys.* **114**, 3765 (2001).
- ⁹M. M. Calbi, F. Toigo, and M. W. Cole, *Phys. Rev. Lett.* **86**, 5062 (2001).
- ¹⁰M. W. Cole, V. H. Crespi, G. Stan, C. Ebner, J. M. Hartman, S. Moroni, and M. Boninsegni, *Phys. Rev. Lett.* **84**, 3883 (2000).
- ¹¹K. A. Williams and P. C. Eklund, *Chem. Phys. Lett.* **320**, 352 (2000).
- ¹²S. Talapatra, A. J. Zambano, S. E. Weber, and A. D. Migone, *Phys. Rev. Lett.* **85**, 138 (2000).
- ¹³S. E. Weber, S. Talapatra, C. Journet, A. Zambano, and A. D. Migone, *Phys. Rev. B* **61**, 13 150 (2000).
- ¹⁴A. J. Zambano, S. Talapatra, and A. D. Migone, *Phys. Rev. B* **64**, 075415 (2001).
- ¹⁵E. B. Mackie, R. A. Wolfson, L. M. Arnold, K. Lafdi, and A. D. Migone, *Langmuir* **13**, 7197 (1997).
- ¹⁶S. Talapatra and A. D. Migone, *Phys. Rev. Lett.* **87**, 206106 (2001).
- ¹⁷S. Inoue, N. Ichikuni, T. Suzuki, T. Uematsu, and K. Kaneko, *J. Chem. Soc. B* **102**, 4690 (1998).
- ¹⁸M. Muris, N. Dufau, M. Bienfait, N. Dupont-Pavlovsky, Y. Grillet, and J. P. Palmari, *Langmuir* **16**, 7019 (2000).
- ¹⁹A. Fujiwara, K. Ishii, H. Suematsu, H. Kataura, Y. Maniwa, S. Suzuki, and Y. Achiba, *Chem. Phys. Lett.* **336**, 205 (2001).
- ²⁰O. E. Vilches, A. Tyburski, T. Wilson, M. Depies, D. Becquet, and M. Bienfait, *Bull. Am. Phys. Soc.* **46**, 1223 (2001).
- ²¹W. Teizer, R. B. Hallock, E. Dujardin, and T. W. Ebbesen, *Phys. Rev. Lett.* **82**, 5305 (1999); **84**, 1844 (2000).
- ²²A. Kuznetsova, J. T. Yates, J. Liu, and R. E. Smalley, *J. Chem. Phys.* **112**, 9590 (2000).
- ²³A. Kuznetsova, D. B. Mawhinney, V. Naumenko, J. T. Yates, J. Liu, and R. E. Smalley, *Chem. Phys. Lett.* **321**, 292 (2000).
- ²⁴A. C. Dillon, K. M. Jones, T. A. Bekkadal, C. H. Kiang, D. S. Bethune, and M. J. Heben, *Nature (London)* **386**, 377 (1997).
- ²⁵A. C. Dillon and M. J. Heben, *Appl. Phys. A: Mater. Sci. Process.* **72**, 133 (2001).
- ²⁶C. Nutzenandel, A. Zuttel, D. Chartouni, and L. Schlapbach, *Electrochem. Solid-State Lett.* **2**, 30 (1999).
- ²⁷M. S. Dresselhaus, K. A. Williams, P. C. Eklund, *Mater. Res. Bull.* **24**, 45 (1999).
- ²⁸C. Journet, W. X. Maser, P. Bernier, M. Lamy de la Chappelle, S. Lefrants, P. Deniards, R. Lee, and J. E. Fischer, *Nature (London)* **388**, 756 (1997).
- ²⁹P. Shrestha, M. T. Alkhafaji, M. M. Lukowitz, G. Yang, and A. D. Migone, *Langmuir* **10**, 3244 (1994).
- ³⁰T. Takaishi and Y. Sensui, *Trans. Faraday Soc.* **53**, 2503 (1963).
- ³¹L. W. Bruch, M. W. Cole, and E. Zaremba, *Physical Adsorption: Forces and Phenomena* (Oxford University Press, New York, 1997).
- ³²A. Thomy and X. Duval, *J. Chimie Physique (Paris)* **67**, 1101 (1970).